

## A FACILE HYDROTHERMAL SYNTHESIS OF MAGNETIC $\text{CoFe}_2\text{O}_4$ NANOPARTICLES AND PHOTOCATALYTIC PERFORMANCE

C. SUWANCHAWALIT\*, V. SOMJIT

*Department of Chemistry, Faculty of Science, Silpakorn University, Sanam Chandra Palace Campus, Nakornpathom, Thailand 73000*

A magnetic cobalt ferrite ( $\text{CoFe}_2\text{O}_4$ ) nanoparticles synthesized via a simple hydrothermal method using  $\text{FeCl}_3 \cdot 6\text{H}_2\text{O}$  and  $\text{CoCl}_2 \cdot 6\text{H}_2\text{O}$  as precursors and glycerol as a stabilizing agent. We have studied the effect of pH on the microstructure and photocatalytic performance of  $\text{CoFe}_2\text{O}_4$  nanoparticles. The prepared samples were characterized by X-ray powder diffraction (XRD), diffuse reflectance UV-vis spectroscopy (DRS), scanning electron microscopy (SEM), Fourier transform infrared spectroscopy (FTIR), and measurement of the surface area using  $\text{N}_2$  adsorption-desorption. The photocatalytic degradation of indigo carmine dye (IC) was evaluated under visible irradiation. The photocatalytic activity was found to be affected by the structural and optical properties as well as the surface area of the samples. The  $\text{CoFe}_2\text{O}_4$  prepared at pH10 exhibited the highest photocatalytic activity for the degradation of indigo carmine dye. The synthesized  $\text{CoFe}_2\text{O}_4$  can be potentially used as a visible-light responsive magnetically separable photocatalyst for wastewater treatment by magnetic separation.

(Received May 5, 2015; Accepted June 22, 2015)

*Keywords:* Cobalt ferrite,  $\text{CoFe}_2\text{O}_4$ , Magnetic nanoparticle, Visible photocatalyst, Degradation of dye

### 1. Introduction

Environmental problems have emerged as global concerns and are associated with industrialization. The utilization of solar energy by semiconductor photocatalysis to solve environmental problems and energy crisis has attracted wide attention [1, 2, 3]. Nano-semiconductor photocatalysts offer an extremely convenient route for eliminating the various organic pollutants can be easily degraded under UV or solar light irradiation in the presence of photocatalysts [1, 2, 4]. The major problem of using the nano-semiconductors is the ability to separate the small sized photocatalysts from the suspensions. In order to overcome this separation problem, magnetic photocatalysts offer an advantage since they can be recovered by applying an external magnetic field.

Among various materials, cobalt ferrite ( $\text{CoFe}_2\text{O}_4$ ) is a well-known spinel magnetic ferrite material due to its strong magnetic anisotropy, moderate magnetization, and high coercivity at room temperature. It is well known that bivalent cation ( $\text{Co}^{2+}$ ) and trivalent ferric ion ( $\text{Fe}^{3+}$ ) can distribute at both tetrahedral and octahedral sites and the type of cationic distribution affects the magnetic properties of spinel ferrite [5, 6]. The presence of  $\text{CoFe}_2\text{O}_4$  magnetic nanoparticles fairly enhances the efficiency of the degradation of organic contaminants which can be easily separated from the solution by applying an external magnetic field.

In this study, spinel  $\text{CoFe}_2\text{O}_4$  photocatalysts were synthesized by utilizing the surfactant-assisted hydrothermal method using  $\text{FeCl}_3 \cdot 6\text{H}_2\text{O}$  and  $\text{CoCl}_2 \cdot 6\text{H}_2\text{O}$  as precursors and sodium hydroxide as a pH adjustor. The effect of preparative pH during the synthesis was studied. The microstructure and optical properties of the synthesized  $\text{CoFe}_2\text{O}_4$  photocatalysts were

---

\*Corresponding author: suwanchawalit\_c@su.ac.th

investigated. The photocatalytic activity of the as-prepared photocatalyst was tested using indigo carmine as a model pollutant.

## 2. Experimental Procedure

### 2.1 Preparation of magnetic $\text{CoFe}_2\text{O}_4$ photocatalyst

All reagents were obtained from commercial sources and used without further purification.  $\text{FeCl}_3 \cdot 6\text{H}_2\text{O}$  and  $\text{CoCl}_2 \cdot 6\text{H}_2\text{O}$  were used as starting precursors, sodium hydroxide (NaOH) as a precipitating agent, and glycerol as a stabilizing agent. In a typical preparation of the magnetic  $\text{CoFe}_2\text{O}_4$ , 4 mmol of  $\text{FeCl}_3 \cdot 6\text{H}_2\text{O}$  was mixed with 0.078 M glycerol under stirring. After mixing well, an aqueous solution of 2 mmol of  $\text{CoCl}_2 \cdot 6\text{H}_2\text{O}$  was slowly added to the above mixture to give a uniform solution. The pH was then adjusted to 10 by dropwise addition of 6 M NaOH aqueous solution. Then the mixture was transferred to a Teflon-lined autoclave and kept at 200 °C in a furnace for 6 h. Finally, the precipitate was collected, centrifuged and washed several times with distilled water then dried at 100 °C for 6 h.

To investigate the influence of pH on the microstructure and the resulting properties, the pHs of the reactions were adjusted to 4, 6, 8, and 12, respectively, keeping these experimental conditions unchanged.

### 2.2 Characterizations

The crystal structure and crystallite size were identified by X-ray diffraction (XRD) patterns recorded on a Rigaku MiniFlex II X-Ray diffractometer with  $\text{Cu K}\alpha$  radiation (1.5406 Å) from 20° to 70° (2 $\theta$ ). Brunauer-Emmett-Teller (BET) surface area measurements were performed on a Quantachrome instrument in  $\text{N}_2$ -adsorption mode. The particle morphologies and microstructure were investigated using a scanning electron microscopy (SEM, JEOL model JSM-5410LV). Fourier-transformed infrared (FT-IR) spectra were recorded on a Perkin Elmer Spectrum Bx spectrophotometer in the range 400–4000  $\text{cm}^{-1}$  using the KBr pellet technique. Optical absorption property and band gap energy were determined using a Shimadzu UV-2401 spectrophotometer.

### 2.3 Photocatalytic experiment

The photocatalytic activities of the prepared  $\text{CoFe}_2\text{O}_4$  samples were evaluated by the photocatalytic degradation of indigo carmine (IC) under visible light using fluorescence light 18W as a visible light source. The photocatalytic experiments were performed at room temperature. A 0.05 g of  $\text{CoFe}_2\text{O}_4$  sample was added to 50 mL IC solution. Prior to the illumination, the suspension was stirred for 1 h to allow adsorption equilibrium of the dye onto the surface of the  $\text{CoFe}_2\text{O}_4$  sample. At given irradiation time intervals, samples were collected and centrifuged to separate  $\text{CoFe}_2\text{O}_4$  powders. The residual concentration of IC was monitored by the change in absorbance of the IC dye at wavelength of 610 nm using a UV-Vis spectrophotometer (Analytik Jena GmbH).

## 3. Results and discussion

The physical property and magnetic separable efficiency of the prepared  $\text{CoFe}_2\text{O}_4$  suspension, shown in Fig. 1, revealed that the samples can be separated from the solution by applying an external magnetic field.

The XRD patterns of the  $\text{CoFe}_2\text{O}_4$  powders at different pH are shown in Fig. 2. As shown in Fig. 2, the  $\text{CoFe}_2\text{O}_4$  samples prepared at pH 4.0 and 6.0 existed in the rhombohedral phase of

$\alpha$ -Fe<sub>2</sub>O<sub>3</sub> (JCPDS no: 89-8103) structure [7] while samples prepared at pH 8.0, 10.0 and 12.0 existed in the CoFe<sub>2</sub>O<sub>4</sub> cubic spinel structure (JCPDS no: 22-1086) [8]. The average sizes of CoFe<sub>2</sub>O<sub>4</sub> crystallite estimated from XRD data using the Scherrer's equation are listed in Table 1. It is clear that the CoFe<sub>2</sub>O<sub>4</sub> nanocrystallite size increased with the preparative pH for both the  $\alpha$ -Fe<sub>2</sub>O<sub>3</sub> and cubic spinel CoFe<sub>2</sub>O<sub>4</sub>.

The nitrogen adsorption–desorption isotherms of the CoFe<sub>2</sub>O<sub>4</sub> powders at different pH (Fig. 3) appear to be of the type IV (BDDT classification), indicating that the mesoporous structure was formed. The surface areas of the synthesized CoFe<sub>2</sub>O<sub>4</sub> samples are shown in Table 1. Moreover, the mesoporous structure could trap photogenerated electrons and holes which enhance the photocatalytic performance.

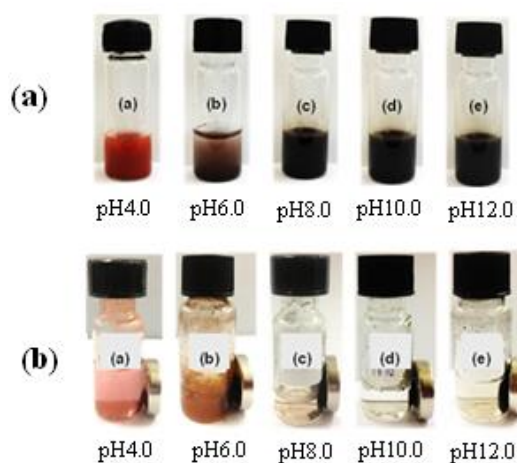


Fig.1 The prepared CoFe<sub>2</sub>O<sub>4</sub> suspension before (a) and after (b) application of the external magnetic field.

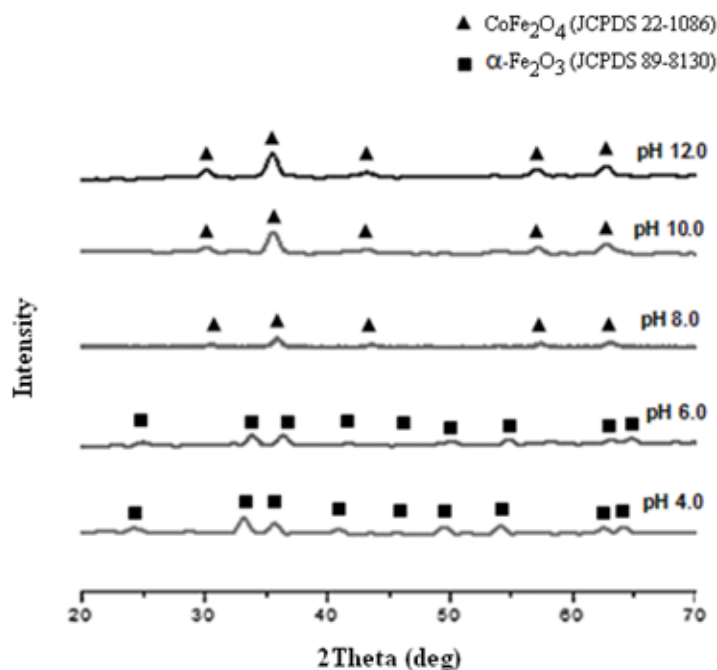
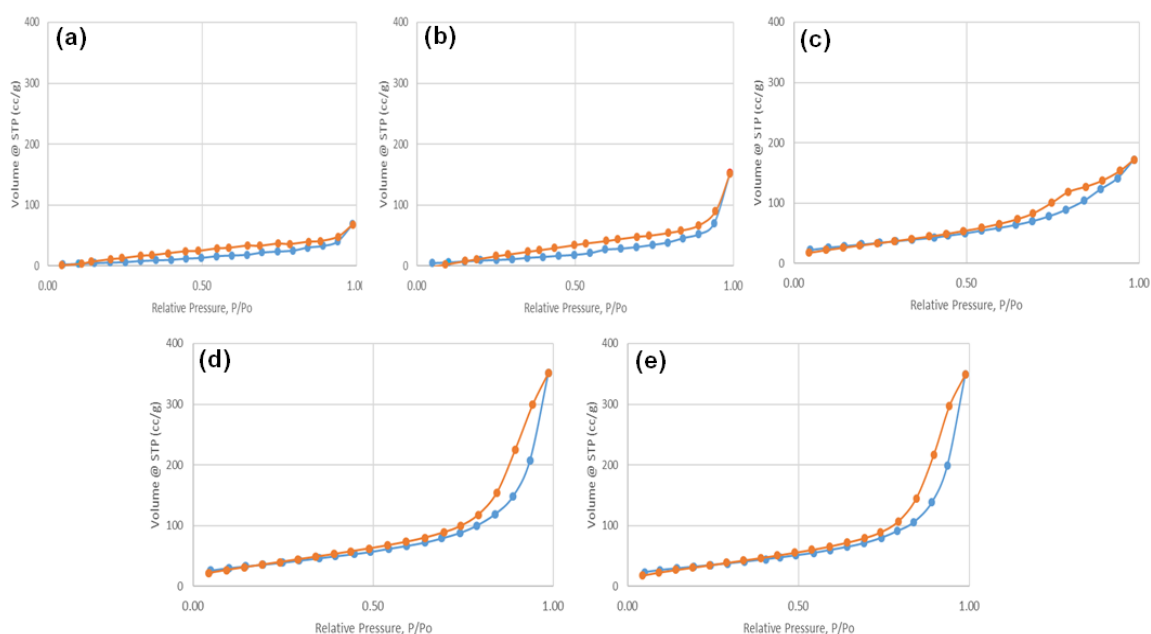


Fig. 2 The XRD patterns of the prepared CoFe<sub>2</sub>O<sub>4</sub> photocatalysts.

Table 1: The calculated crystallite size, specific surface area, and band gap energy of synthesized  $\text{CoFe}_2\text{O}_4$  photocatalysts.

<b><math>\text{CoFe}_2\text{O}_4</math> photocatalysts</b>	<b>Crystallite size (nm)</b>	<b>Surface area (<math>\text{m}^2/\text{g}</math>)</b>	<b>Band gap energy (eV)</b>
$\text{CoFe}_2\text{O}_4$ -pH 4.0	36.88	41	1.68
$\text{CoFe}_2\text{O}_4$ -pH 6.0	28.20	76	1.68
$\text{CoFe}_2\text{O}_4$ -pH 8.0	10.76	119	2.03
$\text{CoFe}_2\text{O}_4$ -pH 10.0	21.27	146	1.75
$\text{CoFe}_2\text{O}_4$ -pH 12.0	19.86	140	1.75



ig. 3 The  $\text{N}_2$  adsorption-desorption isotherm of the prepared  $\text{CoFe}_2\text{O}_4$  photocatalysts.

The morphologies of the  $\text{CoFe}_2\text{O}_4$ , investigated by SEM technique, are shown in Fig. 4. The SEM images reveal that the synthesized  $\text{CoFe}_2\text{O}_4$  samples consisted of spherical particles. The  $\text{CoFe}_2\text{O}_4$  synthesized at pH 8.0 had a spherical shape with the smallest size, consistent with the XRD results. The energy-dispersive X-ray spectroscopy (EDS) analysis, shown in Fig. 5, demonstrates the presence of Co, Fe, and O elements in the  $\text{CoFe}_2\text{O}_4$  sample. The determined atomic ratio of Co: Fe: O in the sample was 1.00: 1.69: 3.81, consistent with the nominal composition.

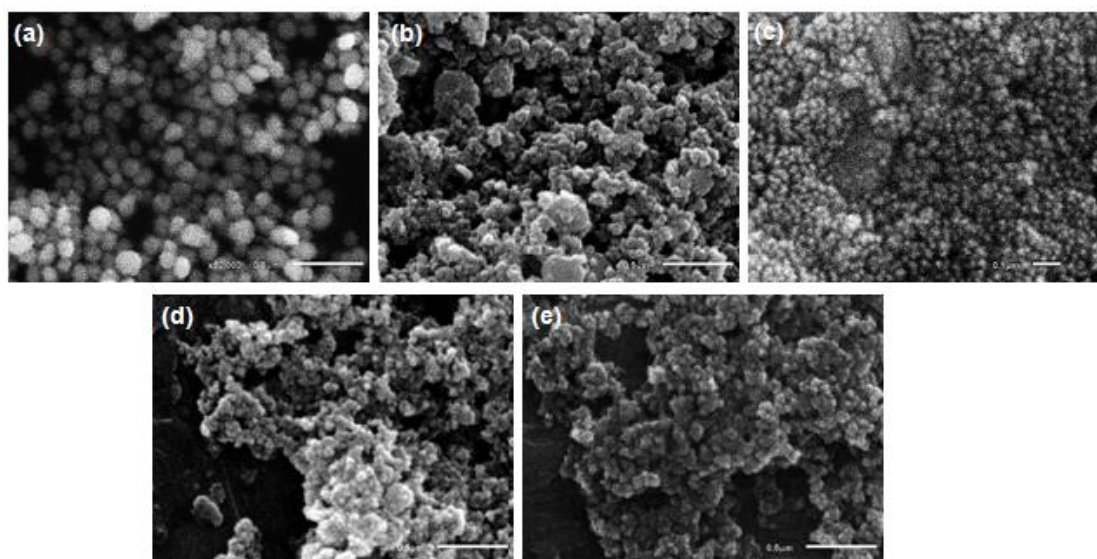


Fig. 4 The SEM images of prepared  $\text{CoFe}_2\text{O}_4$  (a) pH4.0, (b) pH6.0, (c) pH 8.0, (d) pH10.0, (e) pH12.0.

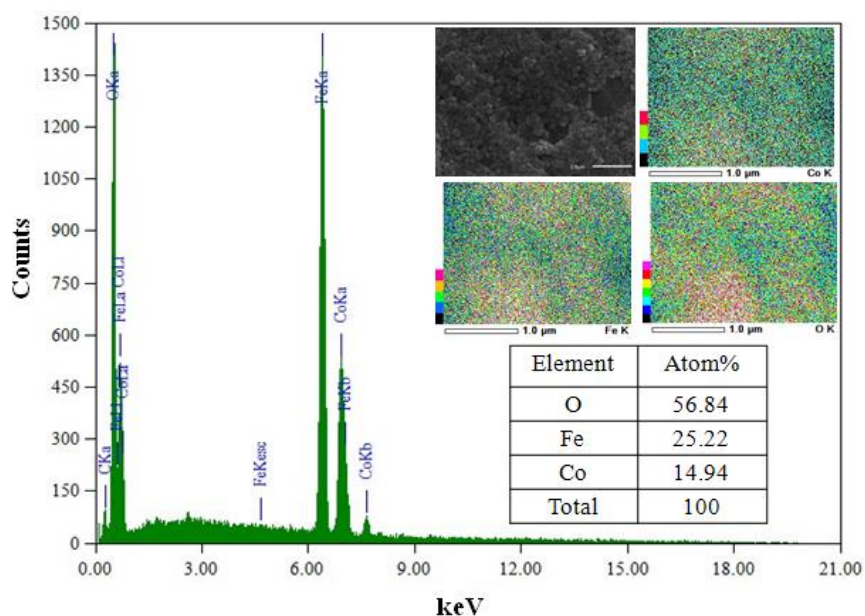


Fig. 5 EDS spectrum of prepared  $\text{CoFe}_2\text{O}_4$ \_pH10.0 sample.

The FT-IR absorption spectra of the prepared  $\text{CoFe}_2\text{O}_4$  samples synthesized at different pH are shown in Fig. 6. The FT-IR spectra of all synthesized  $\text{CoFe}_2\text{O}_4$  samples are consistent with the conclusion from XRD study. Usually, two main broad metal oxygen bonds are seen in the FT-IR spectra of all spinels [9, 10]. The FT-IR bands, observed in the range  $600\text{-}500\text{ cm}^{-1}$ , correspond to the intrinsic stretching vibrations of the metal at the tetrahedral site Co-O stretching vibration band in  $\text{CoFe}_2\text{O}_4$  and Fe-O stretching band in  $\alpha\text{-Fe}_2\text{O}_3$ . Evidences of the octahedral group Fe-O are in the range  $415\text{-}482\text{ cm}^{-1}$ . The bands at  $3500\text{-}3200\text{ cm}^{-1}$  and  $1620\text{ cm}^{-1}$  are attributed to the stretching and bending mode of free and absorbed water on the surface of the synthesized  $\text{CoFe}_2\text{O}_4$  samples.

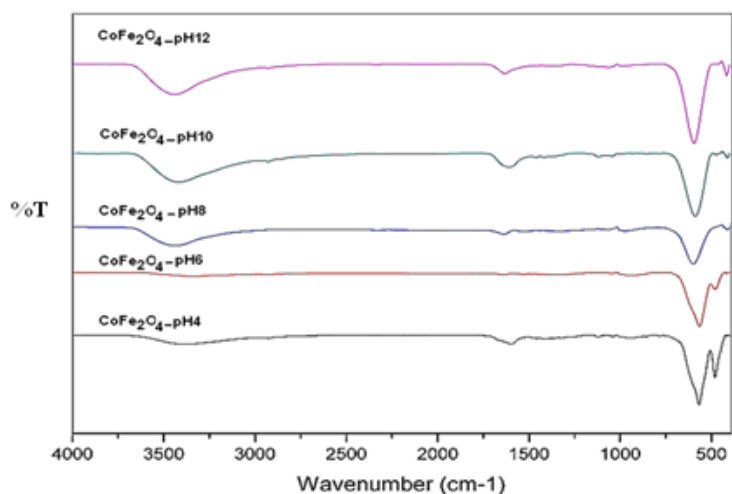


Fig. 6 The FT-IR spectra of the prepared CoFe<sub>2</sub>O<sub>4</sub> photocatalysts.

The optical absorption property relevant to the electronic structure feature is recognized as a key factor in determining the photocatalytic activity [11]. The optical properties of the prepared CoFe<sub>2</sub>O<sub>4</sub> samples were investigated by the diffused reflectance UV-vis spectra (DRS) of the CoFe<sub>2</sub>O<sub>4</sub>, as shown in Figure 6. According to the spectra, all synthesized CoFe<sub>2</sub>O<sub>4</sub> samples exhibited photoabsorption from UV light to visible light region, which implies the possibility of high photocatalytic efficiency of these materials under visible light. The absorption shoulder of the ferrite in the visible region may be attributed to the electron excitation from the O2p level to the Fe3d level for the spinel type compound [12]. The band gap of the synthesized CoFe<sub>2</sub>O<sub>4</sub> calculated from the plot of the transformed Kubelka-Munck function vs. the energy of light [12], is shown in Table 1.

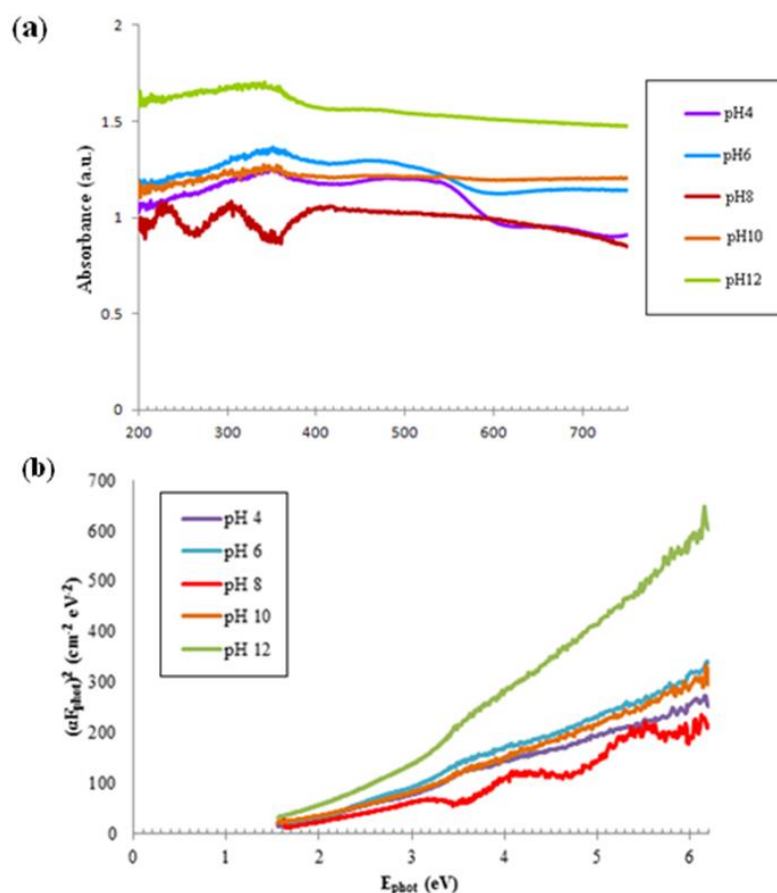


Fig. 7 DRS spectra of (A) prepared CoFe<sub>2</sub>O<sub>4</sub> samples and (B) plots of  $(\alpha h\nu)^2$  vs. photon energy ( $h\nu$ ).

The photocatalytic degradation of indigo carmine dye (IC,  $1.0 \times 10^{-5} \text{M}$ ) as a function of time using the prepared CoFe<sub>2</sub>O<sub>4</sub> samples was investigated under visible light irradiation, as shown in Fig. 8. It can be seen that the CoFe<sub>2</sub>O<sub>4</sub> synthesized at pH 10 gave the best performance in photocatalytic activity of methylene blue. It has been reported that the difference in photocatalytic efficiency could be related to the crystal structure, crystal size, morphology, surface area, and energy band structure [12, 13, 14]. The CoFe<sub>2</sub>O<sub>4</sub> synthesized at pH 10.0 gave the highest photocatalytic efficiency due to the good optical absorptions in UV-Vis region with a lower band gap energy and a larger surface area giving rise to a higher photocatalytic performance. Moreover, the presence of the mesoporous structure could favor the adsorption and diffusion of the dye molecules on the surface of catalyst, thus giving rise to enhanced photocatalytic efficiency of the as-prepared CoFe<sub>2</sub>O<sub>4</sub> samples.

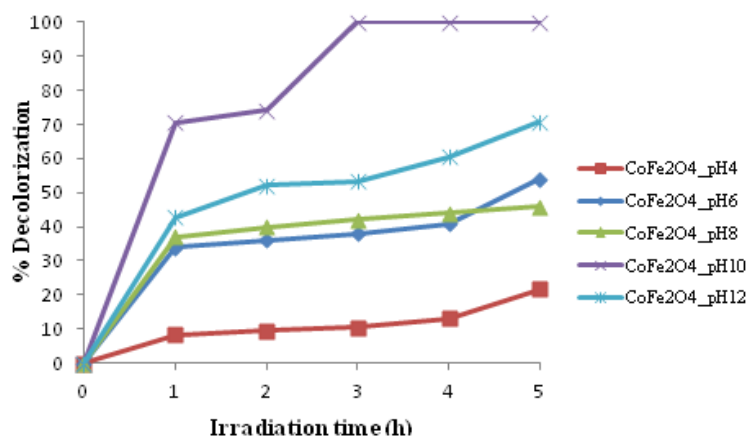


Fig. 8 Photocatalytic degradation of indigo carmine using  $\text{CoFe}_2\text{O}_4$  under visible irradiation.

#### 4. Conclusion

The spinel structure  $\text{CoFe}_2\text{O}_4$  photocatalysts has been successfully synthesized by a one-step hydrothermal method. This method was based on the direct chemical reaction between  $\text{FeCl}_3 \cdot 6\text{H}_2\text{O}$  and  $\text{CoCl}_2 \cdot 6\text{H}_2\text{O}$  with glycerol as a surfactant. Our results reveal that the preparative pHs during the reaction strongly influenced the microstructure and optical properties of the magnetic  $\text{CoFe}_2\text{O}_4$  photocatalysts. The  $\text{CoFe}_2\text{O}_4$ \_pH10 sample showed high photocatalytic activity for the degradation of indigo carmine dyes under visible light irradiation. Moreover, the prepared  $\text{CoFe}_2\text{O}_4$  photocatalysts showed good magnetic response and can potentially be used for cleaning polluted water with the help of magnetic separation.

#### Acknowledgments

This research is supported by the Faculty of Science, Silpakorn University, Thailand (Grant No. SRF-JRG-2557-07). We would like to thank Dr. Supakij Suttiruengwong, Department of Materials Science and Engineering, Faculty of Engineering and Industrial Technology, Silpakorn University for BET measurement.

#### References

- [1] A. Fujishima, K. Honda, *Nature*. **238**, 37 (1972).
- [2] P.V. Kamat, *Chem. Rev.* **93**, 267 (1993).
- [3] H. Li, S.H. Chien, M.K. Hsieh, D.A. Dzombak, R.D. Vidic, *Environ. Sci. Tech.* **45**, 4195 (2011).
- [4] Y.H. Zheng, C.Q. Chen, Y.Y. Zhan, X.Y. Lin, Q. Zheng, K.M. Wei, J.F. Zhu, *J. Phys. Chem. C*. **112**, 10773 (2008).
- [5] Z. Zi, Y. Sun, Z. Yang, J. Dai, W. Song, *J. Magn.Magn. Mater.* **321**, 1251 (2009).
- [6] X.Cao, L. Gu, *Nanotechnology*, **16**, 180 (2005).
- [7] R. Satheesh, K. Vignesh, A. Suganthi, M. Rajarajan, *J. Environ. Chem. Eng.* **2**, 1956 (2014).
- [8] S. Rohilla, S. Kumar, P. Aghamkar, S. Sunder, A. Agarwal, *J. Magn.Magn. Mater.* **323**, 897 (2011).
- [9] P. Vlazan, M. Stefanescu, P. Barvinschi, M. Stoia, *Mater. Res. Bull.* **47**, 4119 (2012).

- [10] N. Li, M. Zheng, X. Chang, G. Ji, H. Lu, L. Xue, L. Pan, J. Cao, J. Solid State Chem. **184**, 953 (2011).
- [11] P. Sathishkumar, R.V. Mangalaraja, S. Anandan, M. Ashokkumar, Chem. Eng. J. **220**, 302 (2013).
- [12] H. Guo, J. Chen, W. Weng, Q. Wang, S. Li, Chem. Eng. J. **239**, 192 (2014).
- [13] E. Casbeer, V.K. Sharma, X.Z. Li, Sep. Purif. Technol. **87**, 1 (2012).
- [14] X. Li, Y. Hou, Q. Zhao, L. Wang, J. Colloid Interface Sci. **358**, 102 (2011).